Validation of a Model and of a Simulator for Road Cycling on Real Tracks*

Thorsten Dahmen, Roman Byshko, Dietmar Saupe
University of Konstanz, Germany

Martin Röder
ND SatCom GmbH, Immenstaad, Germany

Stephan Mantler
VRVis Center for Virtual Reality and Visualization Research, Vienna, Austria

Abstract

Methods for data acquisition, analysis, and modelling of performance parameters in road cycling have been developed. A simulator to facilitate the measurement of training parameters in a laboratory environment has been designed as well as models for performance prediction. The simulation includes real height profiles and a video playback that is synchronised with the cyclist's current virtual position on the track and online visualisation of various course and performance parameters. Field data obtained in this study were compared with the state-of-the art mathematical model for road cycling power, established by Martin et al. in 1998, which accounts for the gradient force, air resistance, rolling resistance, frictional losses in wheel bearings, and inertia. The model was able to describe the performance parameters accurately with correlation coefficients of 0.87–0.95. This study showed that the mathematical model can be implemented on an ergometer for simulating rides on real courses. Comparing field and simulator measurements gave correlation coefficients between 0.66–0.81.

1 Introduction

Computer science in sports is an emerging interdisciplinary field, which has evolved in the last 20 to 30 years focussing on the following areas of research: data acquisition, processing and analysis, modelling and simulation, data bases and expert systems, multimedia and presentation, and IT networks/communication [3]. Recording devices for a host of physical and physiological parameters have become available both to the professional athlete as well as to non-professional sportsmen. These parameters are used for monitoring and measuring sports activities in the lab, during training and even in competition. However, after the data have become available, it still remains difficult to efficiently extract the relevant information. In our work we contribute to the research aimed at the entire cycle of data acquisition, filtering, analysis, visualisation, modelling, and prediction of such complex data. We selected endurance sports as a particularly suitable application since it allows for long-term data series that are expected to be more homogeneous, and that depend to a lesser degree on chance events than, e.g., in game sports. Currently our work focuses on road cycling, that may later be extended to include, e.g., running and rowing.

For road cycling we develop methods for data acquisition, analysis, modelling and visualisation of performance parameters. We designed a simulator to facilitate the measurement of training parameters in a laboratory environment in addition to measuring performance parameters in the field [11]. Several mathematical models have been introduced to model road cycling performance, e.g., [5, 8, 9, 10]. These models were derived from the equilibrium of energy demands and supplies. The state-of-the art mathematical model for road cycling power, established by Martin et al. in 1998 [8], accounts for the gradient force, air resistance, rolling resistance, frictional losses in wheel bearings, and inertia. The models were used to predict time trial performance [10] and required power output during cycling [8]. Mathematical performance models were also used to derive optimal pacing strategies for time trials in variable synthetic terrain and wind conditions [1, 2, 6, 7].

This paper focusses on a comparison of performance parameters in the field, on our lab simulator, and those produced by the mathematical model. Previously, validations of mathematical models for cycling performance were performed by comparing predictions of the models to measurements on a flat course. For this study we chose two uphill tracks with varying steepness. Specifically, the cyclist's climbing progress on real outdoor rides on these tracks together with measurements of a power meter is compared to predictions of the mathematical model for these tracks.

*This research was supported by the DFG Research Training Group GRK 1042, "Explorative Analysis and Visualization of Large Information Spaces". The paper has been presented at the 7th International Symposium on Computer Science in Sport, Canberra, 22–25 September, 2009. A revised version of this document will be submitted for publication.

Another contribution of this paper is the comparison between performance parameters measured by the simulator and those calculated by the mathematical model. The main purpose of this task is to provide a means to evaluate the extent to which a lab ergometer ride can accurately simulate an outdoor ride on real-world tracks. Such simulations may then be used by athletes to prepare for competitions on unknown courses.

In the following subsection we outline the mathematical model for cycling power that we used for our comparison with field and lab tests. In Section 2 we discuss the cycling courses, the equipment, the test setup, the data preprocessing, and the means of comparison of measurements and model prediction. The following three sections include the results, their discussion, and conclusions.

1.1 The mathematical model

Beginning in the 1980s, mathematical models have been developed to describe the relation between pedalling power and velocity with road cycling. Although these models comprise a multitude of physical phenomena, their accuracy could not be determined before the SRM Training system [12] became available commercially in 1994. Then, in 1998 Martin et al. summarised the significant components to form a mathematical model for road cycling power and successfully validated it, [8]. They compared outdoor measurements of the SRM system on a flat road with different constant velocities to power predictions derived from the model, which accounted for over 97% of the variation of cycling power.

The model is based on Newtonian mechanics, as an equilibrium of resistance power and pedalling power P_{ped} provided by the cyclists to propel his bicycle. The resistance power is composed of power due to gain in potential energy P_{pot}, aerodynamic drag P_{air}, frictional losses in wheel bearings P_{bear}, rolling friction P_{roll}, and gain in kinetic energy P_{kin},

$$P_{\text{pot}} + P_{\text{air}} + P_{\text{bear}} + P_{\text{roll}} + P_{\text{kin}} = \eta P_{\text{ped}} \,. \tag{1}$$

The efficiency factor $\eta < 1$ accounts for frictional loss in the drive chain.

Dividing this equation by the angular velocity of the wheels yields the corresponding equilibrium of torques where we have to consider the lever principle using the transmission ratio $\gamma = \frac{n_{\text{front}}}{n_{\text{rear}}}$, i.e., the ratio of the number of teeth on the front sprocket to the number of teeth on the rear sprocket:

$$T_{\text{pot}} + T_{\text{air}} + T_{\text{bear}} + T_{\text{roll}} + T_{\text{kin}} = \frac{\eta}{\gamma} T_{\text{ped}} \,. \tag{2}$$

The pedal torque is equal to the product of the pedal force and the length of the crank: $T_{\text{ped}} = F_{\text{ped}} l_c$. Moreover, we divide Equation (2) by the radius of the wheels, r_w, in order to obtain the decomposition of resistance forces on the left hand side, (3). These forces act at the contact area between the rear wheel and the road.

$$F_{\text{pot}} + F_{\text{air}} + F_{\text{bear}} + F_{\text{roll}} + F_{\text{kin}} = \frac{\eta}{\gamma} \frac{l_c}{r_w} F_{\text{ped}} \,. \tag{3}$$

Eventually, we substitute the specific mechanical models into each component:

$$\underbrace{mg\frac{\partial h}{\partial x}}_{F_{\text{pot}}} + \underbrace{\frac{1}{2} c_d \rho A \dot{x}^2}_{F_{\text{air}}} + \underbrace{(\beta_0 + \beta_1 \dot{x})}_{F_{\text{bear}}} + \underbrace{\mu m g}_{F_{\text{roll}}} + \underbrace{\left(m + \frac{I_w}{r_w^2}\right)\ddot{x}}_{F_{\text{kin}}} = \frac{\eta}{\gamma} \frac{l_c}{r_w} F_{\text{ped}} \tag{4}$$

Here, $x = x(t)$ is the distance travelled as a function of time t, $\dot{x} = v(t)$ is the velocity, and $\ddot{x} = \dot{v}(t)$ is the acceleration. The other physical parameters are listed in Table 1. For our purposes, we neglect ambient wind and aerodynamic drag caused by rotation of spokes.

Table 1: Physical parameters of the mathematical model. These parameters originate from our own measurements or were taken from the literature as follows: m_c, m_b weighted with scales; I', l_c manufacturer information; $c_w, L, s(x)$ measured using GPS functionality of Garmin Edge 705 device; $I_w, \beta_0, \beta_1, \eta$ from [8]; c_d, A average value from [13], μ standard value from Cyclus2 for asphalt road.

Cyclist/bicycle/simulator		
mass cyclist	m_c	Tab. 3
mass bicycle	m_b	10.6 kg
total mass	m	$m_b + m_c$
simulator inertia	I'	$0.543\,\text{kgm}^2$
wheel circumference	c_w	2100 mm
wheel radius	r_w	$(2\pi)^{-1} c_w$
wheel inertia	I_w	$0.14\,\text{kgm}^2$
cross-sectional area	A	$0.4\,\text{m}^2$
length of crank	l_c	175 mm
bearing coefficient	β_0	0.091 N
bearing coefficient	β_1	$0.0087\,\text{Ns/m}$
mechanical gear ratio, bicycle	γ	39/26, ..., 53/12
fixed gear ratio, simulator	γ'	53/13
simulated gear ratio	γ'_{sim}	39/26, ..., 53/12
Course/environment		
friction factor	μ	0.004
gravity factor	g	$9.81\,\text{m/s}^2$
drag coefficient	c_d	0.7
air density	ρ	$1.2\,\text{kg/m}^3$
length	L	Tab. 2
height	$h(x)$	Subsec. 2.1
chain efficiency	η	0.975

Thus, the sought relation can be rewritten as a nonlinear differential equation of the form

$$\gamma \frac{r_w}{l_c} f(x(t), \dot{x}(t), \ddot{x}(t)) = \eta F_{\text{ped}}(t) \,, \tag{5}$$

respectively,

$$f(x(t), \dot{x}(t), \ddot{x}(t)) \cdot \dot{x}(t) = \eta P_{\text{ped}}(t) \ , \tag{6}$$

where the discounted pedalling force $\eta F_{\text{ped}}(t)$, respectively the discounted pedalling power $\eta P_{\text{ped}}(t)$, occurs as the driving term for the covered distance $x(t)$, as the independent variable, and $f(x, \dot{x}, \ddot{x})$ denotes the left hand side of Equation (4).

The mathematical model was used in two ways.

1. Given the distance measurements $x(t)$ for the duration of a ride, we computed the corresponding pedalling forces $F_{\text{ped}}(t)$, respectively pedalling power P_{ped}, by evaluating $f(x(t), \dot{x}(t), \ddot{x}(t))$ in Equation (5). These values were then compared with the actual power measurements provided by the SRM.

2. Given measured or prescribed pedalling power $P_{\text{ped}}(t)$ for the duration of a ride, we solved Equation (6) for $x(t)$ numerically (using MATLAB's ode45 function). The derived values for the velocity $v(t) = \dot{x}(t)$ were then compared with the actual velocity measurements provided by the SRM.

For the model with the simulator, we agree on using primed quantities in the following. Here, the cyclist pedals against the power of the eddy current brake P'_{brake}, the power due frictional losses in the bearings (P'_{bear}), to changes of kinetic energy of the flywheel P'_{kin}, and frictional losses in the chain (factor η):

$$P'_{\text{brake}} + P'_{\text{bear}} + P'_{\text{kin}} = \eta P'_{\text{ped}} \ . \tag{7}$$

In analogy to Equations (2) and (3), we write the equilibrium in terms of torques

$$T'_{\text{brake}} + T'_{\text{bear}} + T'_{\text{kin}} = \frac{\eta}{\gamma'} T'_{\text{ped}} \ , \tag{8}$$

and in terms of forces

$$F'_{\text{brake}} + F'_{\text{bear}} + F'_{\text{kin}} = \frac{\eta}{\gamma'} \frac{l_c}{r_w} F'_{\text{ped}} \ . \tag{9}$$

Again, we can insert the specific mechanical models:

$$F'_{\text{brake}} + \underbrace{(\beta_0 + \beta_1 \dot{x})}_{F'_{\text{bear}}} + \underbrace{\frac{I'}{r_w^2} \dot{x}}_{F'_{\text{kin}}} = \frac{\eta}{\gamma'} \frac{l_c}{r_w} F'_{\text{ped}} \ . \tag{10}$$

Here, we assume that the frictional losses, represented by β_0 and β_1, are the same as with the bicycle. In fact, their contribution is so small that we could neglect them. The moment of inertia of the ergometer's flywheel I' corresponds to a combined inertial mass of cyclist and bicycle of $m'_i = \frac{I'}{r_w^2} \approx 4.86\,\text{kg}$, which is – as with most ergometers – by far too low.

The ergometer enables us to impose an arbitrary brake torque T'_{brake} with our own control software. In order to simulate real courses, we use the physical models to compute a *simulated* brake torque $T'_{\text{sim,brake}}$ as the sum of simulated torques due to gain in potential energy $T'_{\text{sim,pot}}$, aerodynamic drag $T'_{\text{sim,air}}$, and rolling resistance $T'_{\text{sim,roll}}$. Furthermore, we want to simulate arbitrary gears without any mechanical changes. Therefore, we introduce a factor γ'_{sim} that represents virtual gears and incorpoate it together with the simulated brake torque into the controlled brake torque T'_{brake} of the ergometer. The mechanical gear ratio remains fixed ($\gamma' = \frac{53}{13}$) at all times.

$$\begin{aligned} T'_{\text{brake}} &= \gamma'_{\text{sim}} T'_{\text{sim,brake}} \\ &= \gamma'_{\text{sim}} \left(T'_{\text{sim,pot}} + T'_{\text{sim,air}} + T'_{\text{sim,roll}} \right) \ . \end{aligned} \tag{11}$$

However, we want to ensure that the power that is absorbed by the brake matches the simulated power for gain in potential energy, aerodynamic drag and rolling resistance.

$$P'_{\text{brake}} = P'_{\text{sim,pot}} + P'_{\text{sim,air}} + P'_{\text{sim,roll}} \ . \tag{12}$$

Therefore, we recalculate the angular velocity in the simulation ω'_{sim} which then differs from the angular velocity of the ergometer's flywheel ω':

$$\omega'_{\text{sim}} = \frac{P'_{\text{brake}}}{T'_{\text{brake}}} = \frac{\gamma'_{\text{sim}}}{\gamma'} \omega' \ . \tag{13}$$

This clearly affects the simulated torques due to kinetic energy $T'_{\text{sim,kin}}$. These aspects will be a subject of a future publication. In the following experiments and computations they play only a minor role. With constant velocity, power due to changes in kinetic energy vanishes and in all other model computations for the simulator we accounted for these effects using Newtonian mechanics. Frictional losses in the wheel bearings are much smaller than all other components, so we can expect a negligible error if we assume that they are the same for the bicycle, the ergometer and in our simulation.

2 Methods

2.1 Courses

We selected two uphill courses of about 3 km length, with an ascent of about 250 m each and varying steepness, namely the Schiener Berg and Ottenberg, located near Radolphzell, Germany, and Weinfelden, Switzerland, respectively. See Table 2 and Figures 1–2 for details and picture overviews of the courses. The tracks were recorded by a video camera simultaneously together with the corresponding altitude and GPS tracks with a sampling rate of 1 per second. This allowed us to geo-reference each individual video frame. From this alignment we calculated for each frame the distance travelled from the starting point of the course, the altitude above sea level, and the road gradient. The gradient is given by $s(x) = \tan \arcsin(\frac{\partial h}{\partial x})$. Likewise, for an arbitrary position on the track with a

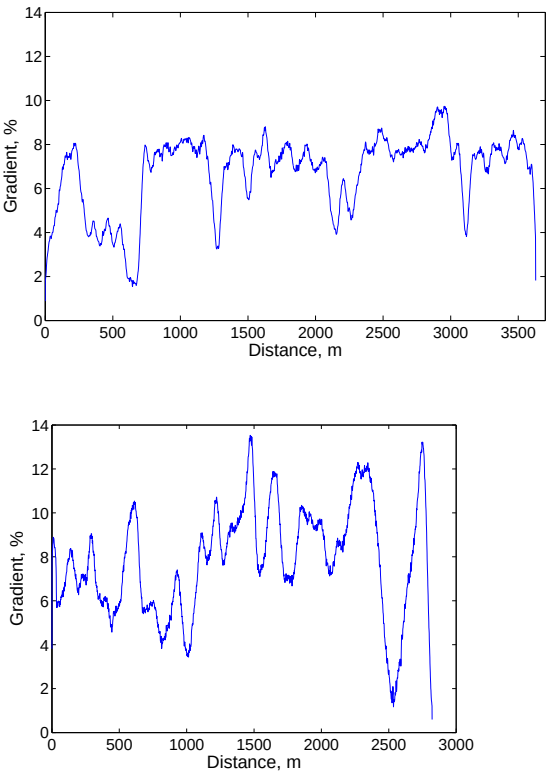

Figure 1: Gradient versus distance of the courses Schiener Berg (left) and Ottenberg (right). The gradient is smoothed with a Gaussian filter ($\sigma = 30\,\mathrm{m}$).

given distance from the starting point one may calculate a corresponding (fractional) video frame number for display in the simulation setting [11].

2.2 Equipment

The riders used the same standard road race bicycle (Radon RPS 9.0 with a 60 cm frame), both in the field and on the simulator. The bicycle has a 10-speed cassette (13–19 and 21, 23, 26 teeth) and is equipped with an SRM power meter with four strain gauge strips (Schoberer Rad Messtechnik, Jülich, Germany) attached to the chain wheel (53, 39 teeth). Such devices for measuring power are considered state-of-the-art and have been validated in [8].

Table 2: Two courses, called Schiener Berg and Ottenberg were chosen for the tests.

	Schiener Berg	Ottenberg
Distance	3630 m	2820 m
Start height	429 m	441 m
End height	674 m	664 m
Average gradient	6.7%	7.9%
Maximum gradient	9.7%	13.5%
Standard deviation of gradient	1.7%	2.5%

Figure 2: Screenshot of simulation program window. Scene from the Schiener Berg course.

In our studies, the SRM measurements for distance travelled, velocity, and power were recorded and used. In addition, other parameters (heart rate, pedalling frequency) were also recorded but not used here.

Our simulator is based on a Cyclus2 ergometer (RBM Elektronik-Automation GmbH, Leipzig, Germany). It allows to mount the user's personal bicycle and has a flexible front axle attachment, thus, providing a realistic cycling experience, also when riding out of the saddle. The ergometer is governed by an eddy current brake which can be directly controlled by an external PC-based software at a 2 Hz rate. In the so-called slave mode we can have the ergometer simulated an appropriate braking action. Our system makes use of this control in order to fully implement the effects of the actual real-world gradient-induced forces, and forces due to aerial drag, and rolling resistance. Inertial forces and frictional losses in the wheel bearings are accounted for by the ergometer mechanics.

In addition we implemented an option that lets the system set virtual gears exactly as given by the 20-speed road bicycle even though the ergometer is designed to accommodate the mechanical gears like those that come with the user's bicycle. These "soft gears" were necessary because the ergometer is not capable to generate large braking forces at low (simulated) velocities, i.e., in low mechanical gears and with a low back wheel angular velocity, as it would be realistic at the very steep sections of the courses. Instead, a (constant) higher mechanical gear is used throughout leading to a high angular velocity requiring a prescribed lower than the real brake force.

The simulation includes a video playback that is synchronised with the cyclist's current position on the track and online visualisation of various course and performance parameters, namely the time since the start of the ride, the distance travelled, the current velocity, road gradient, pedalling frequency, heart rate, gear ratio, power output, and average power output. Moreover, the height profile for the

Figure 3: 3D view of the courses: Schiener Berg (left), Ottenberg (right).

whole course and a plot of the gradient near the current position of the rider is shown. This visual feedback was displayed during the simulated rides in the lab using an LCD projection unit onto a screen of size of about 1 m^2, Figure 2. The details of our simulation system have been presented at [4] and will be published elsewhere. As for the outdoor rides the same parameters were recorded using the mounted SRM chain wheel. Moreover, the Cyclus2 also provided the measurements of the same parameters.

2.3 Field and simulation tests

The two selected courses were ridden by several riders of differing age, weight and training level, including hobby, amateur and competitive cyclists. Each ride was performed on the real course as well as with the simulator in the lab. Since the objective of the experiments was to compare the model predictions for power respectively for velocity with the performance on the road and in the lab, the riders were instructed to try to maintain either a prescribed constant velocity or constant power for each run.

Table 3: Cyclists in the study.

	Age (yrs.)	Weight (kg)	Sex	Experience
A	24	78.6	male	novice cyclist
B	29	73.8	male	occasional cyclist
C	27	91.0	male	occasional cyclist
D	55	73.2	male	hobby cyclist
E	31	60.5	male	amateur cyclist

2.4 Data preprocessing of outdoor measurements

In order to compare the measured power or velocity during an uphill ride with the corresponding model prediction the road gradient for each data point was needed, which was taken from height profiles generated separately. The height profiles were measured with a GPS device mounted on a bicycle (a Garmin Edge 705) slowly pushing the bicycle up the hills. The elevation measurement were noisy and, thus, filtered by a Gauss filter with $\sigma = 30\,\mathrm{m}$. Finally, each elevation was associated with the corresponding measured distance from the defined starting point of the ride.

To look up the road gradient for a given point of an actual ride one has to take the distance travelled from the start, look up the corresponding altitudes in the preprocessed height profiles and estimate a gradient. There are two practical problems to carry out this task.

- The distances measured on the rides by the SRM differed slightly from those in the height profiles. There are several reasons for that. The riders did not ride along the exact same path on the road, and the distances measured for the height profile had been obtained with a device partly based on (noisy) GPS data while on the actual rides only wheel revolutions were automatically counted and multiplied by the wheel circumference to obtain the travelled distance.
- The points for the start and end of the tracks were difficult to locate in the measurement log files because they cannot be exactly marked by the riders when passing them.

To solve both problems jointly, we propose to scale and

translate the height profile to match the measured distances. We did this manually with a computer program as follows. Two parameters, namely the start and end position in the log data, had to be searched for. We identified them by the best match of the measured power curves with the corresponding predicted power curve of the mathematical model, which was obtained by visual comparison together with computed correlation coefficients. This worked for both types of rides, i.e., with constant velocity and with constant power. In the second case we could compare the measured velocity with the velocity that the model predicts using the measured power. This semi-automatic procedure provided good results. We thus refrained from an automated correlation analysis to determine optimal start and end positions.

2.5 Comparison of measurements with model prediction

As result of the preprocessing of the data measured in the field we achieved time series of vectors with the components: time t, distance $x(t)$, velocity $\dot{x}(t)$, power $P_{\mathrm{ped}}(t)$, and gradient $s(x(t))$. For evaluating the rides with constant velocity, these values (except $P_{\mathrm{ped}}(t)$), inserted in the left side of the model equation (6), yield the predicted power for comparison with the measured power. In the Section 3 we provide corresponding graphs and give correlation coefficients and signal-to-noise ratios (SNR). The latter are defined as

$$\mathrm{SNR} = 10 \log_{10} \frac{\mathrm{MSP}_{\mathrm{ped}}}{\mathrm{MSE}} \mathrm{dB} \tag{14}$$

where $\mathrm{MSP}_{\mathrm{ped}}$ and MSE denote the mean square power amplitude and the mean square error between the prediction and the actual power, respectively, measured in decibel. From the SNR we compute the percentage p of the variation of the data that is accounted for by the model as follows,

$$p = 100 \left(1 - \frac{\mathrm{MSE}}{\mathrm{MSP}_{\mathrm{ped}}} \right) \% \, . \tag{15}$$

For evaluating the rides with approximately constant power we simply reversed the roles of velocity and power in the above and define the SNR and percentage p accordingly.

For the analysis of the data obtained with the simulator we proceeded similarly. Since the measured velocity and power data were automatically linked to the used height profiles no preprocessing to align gradients to the measurements was required. The modified model equation (9) was used in place of Equation (3) as the basis of the computations.

2.6 Comparison of simulated rides with outdoor rides

Let us consider a comparison of the field rides with constant velocity with corresponding simulations in the lab. Two steps are required as a preprocessing.

1. Since distances in the field and in the simulations are not exactly identical as discussed further above, we scaled the distances in the field to match those used in the simulator. Care had to be taken so that the velocities are modified accordingly.

2. For comparison of power output the velocities in the field and in the simulator should be identical, but naturally they differed. We propose to use the model to estimate the power output assuming the preset constant velocities, e.g., $v^\star = 10$ km/h.

The compensation for variable velocity proceeds as follows. At each point in time the model for the field resp. the simulator predicts a pedaling power $P^m_{\mathrm{ped}} = P^m_{\mathrm{ped}}(x(t), \dot{x}(t), \ddot{x}(t))$. For constant prescribed velocity $v^\star$, however, the model would predict at that same location of the course a value of $P^\star_{\mathrm{ped}} = P^m_{\mathrm{ped}}(x(t), v^\star, 0)$. Then we can compensate the measured power for the mismatch of the velocity simply by multiplying with the factor $P^\star_{\mathrm{ped}}/P^m_{\mathrm{ped}}$. The compensation must be applied to the measured data from both the field and the simulation. We call the resulting time series the *normalised* power sequences. For rides with attempted constant power we proceeded likewise, normalising the velocity to exactly constant power. The resulting normalised power resp. velocity was then compared using the same methods as described in the last subsection.

3 Results

To gain a view of the contributions of the components of the overall work required to perform a ride on one of the courses we calculated the average powers, $\bar{P}_{(\cdot)}$, and the corresponding fractions that account for gain in potential energy $\bar{P}_{\mathrm{pot}}$, aerodynamic drag $\bar{P}_{\mathrm{air}}$, frictional losses in wheel bearings $\bar{P}_{\mathrm{bear}}$, rolling friction $\bar{P}_{\mathrm{roll}}$, and gain in kinetic energy $\bar{P}_{\mathrm{kin}}$. For our lightest rider (rider E) at the highest approximately constant velocity ($v^\star = 17\,\mathrm{km/h}$) on the Mountain A the average power was 253.8 W, which was distributed as given in Table 4. The total work was 54.2 Wh. It is clear that the fraction due to overcoming the potential energy $\bar{P}_{\mathrm{pot}}$ is dominant while the others are small or even negligible ($\bar{P}_{\mathrm{bear}}$). The average power due to changes of kinetic energy vanishes perfectly. For other (heavier) riders and for lower velocity the fraction for overcoming potential energy on this course was even higher.

In order to present the main results we chose four bicycle rides that are representative and cover different subjects, courses and pacing strategies out of the 17 that were obtained both outdoors on a real course and indoors on the simulator using the same course and pacing. Three of these selected rides were performed with approximately constant velocity $v^\star$ and power was computed using the model. For the fourth one, having approximately constant

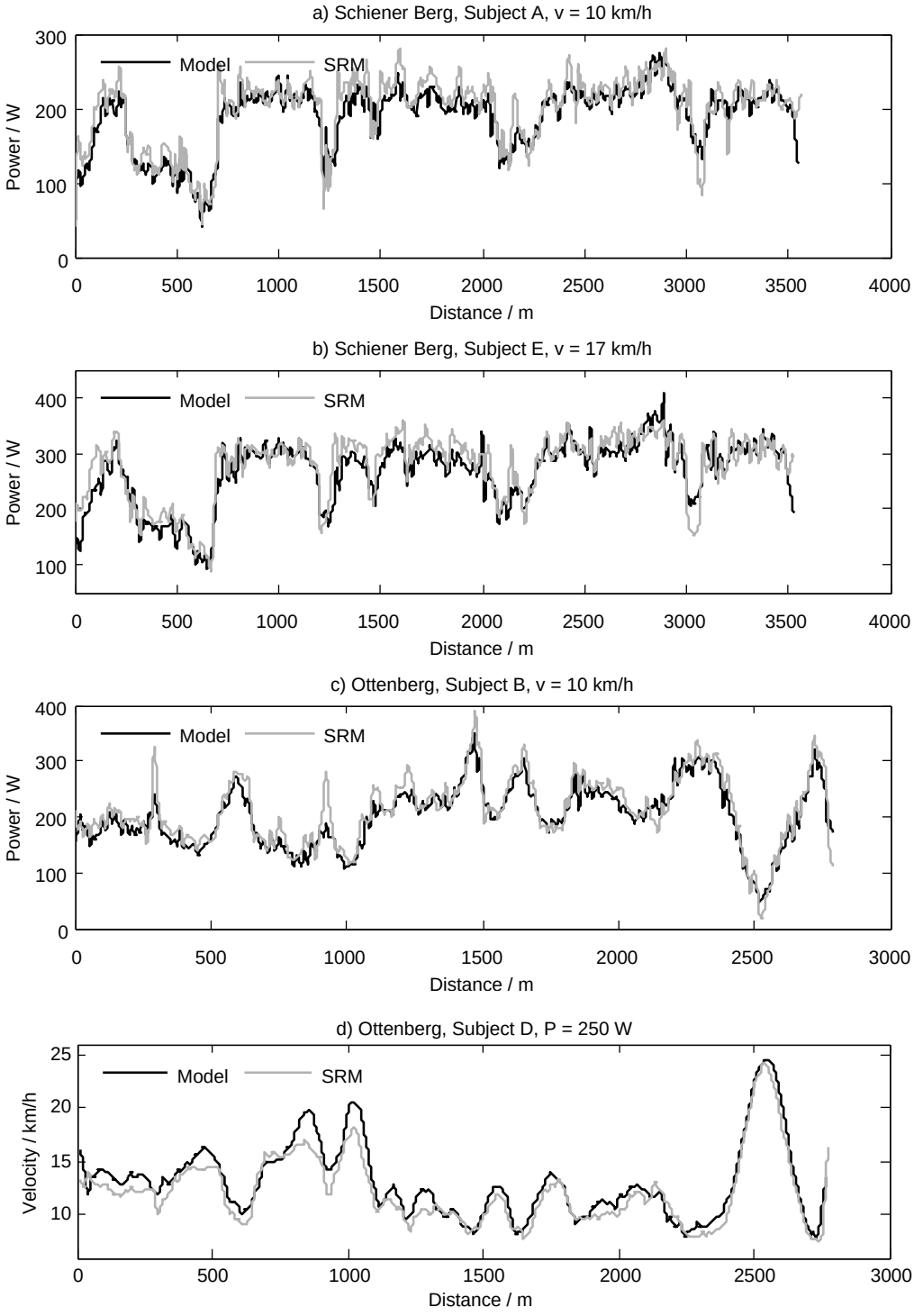

Biker	Condition	Course	ρ	m_e	σ_e	SNR	p
A	$v^\star = 10\,\mathrm{km/h}$	Mountain A	0.87	-9.3 W	24.2 W	18.0 dB	98.8%
E	$v^\star = 17\,\mathrm{km/h}$	Mountain A	0.88	-10.9 W	28.9 W	19.3 dB	98.8%
B	$v^\star = 10\,\mathrm{km/h}$	Mountain B	0.92	-14.0 W	17.9 W	18.2 dB	98.4%
D	$P^\star = 250\,\mathrm{W}$	Mountain B	0.95	$0.23\,\mathrm{km/h}$	$0.28\,\mathrm{km/h}$	19.2 dB	98.5%

Figure 4: Field rides versus model predictions. The solid line in each plot gives the power resp. velocity prediction of the model. The prediction errors are analysed in the table. ρ is the correlation coefficient, σ_e is the standard deviation of the prediction error, SNR is the signal-to-noise ratio, and p the percentage of variation explained by the model. In this table the mean error m_e is the predicted average power resp. velocity minus the average measured power resp. velocity. Note that in the first three lines power is compared, while in the last line velocity is compared.

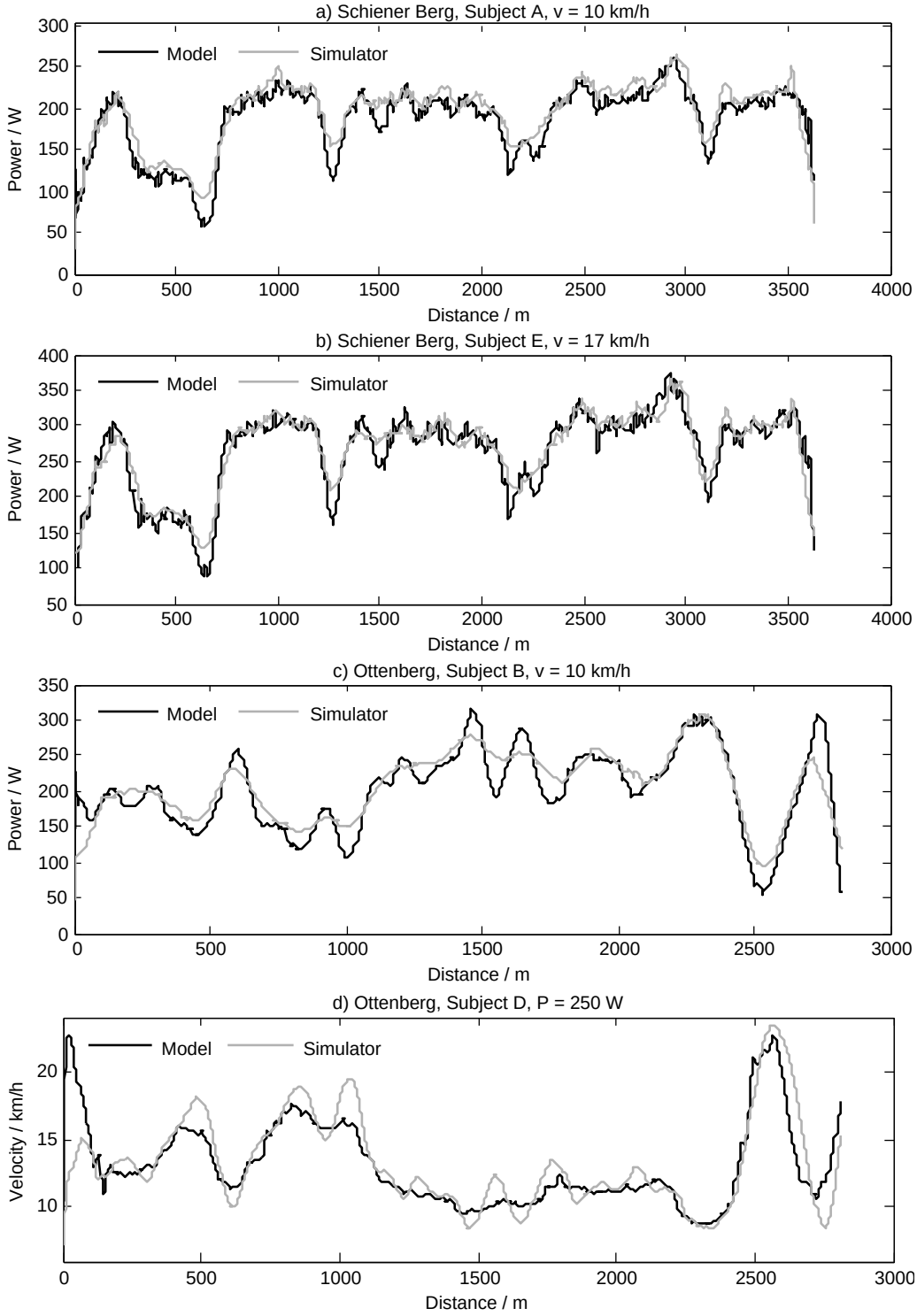

Biker	Condition	Course	ρ	m_e	σ_e	SNR	p
A	$v^\star = 10\,\mathrm{km/h}$	Mountain A	0.90	-8.4 W	18.7 W	19.7 dB	98.9%
E	$v^\star = 17\,\mathrm{km/h}$	Mountain A	0.93	-4.2 W	22.0 W	21.7 dB	99.3%
B	$v^\star = 10\,\mathrm{km/h}$	Mountain B	0.88	-5.2 W	29.0 W	17.7 dB	98.3%
D	$P^\star = 250\,\mathrm{W}$	Mountain B	0.80	-0.005 km/h	0.52 km/h	16.7 dB	97.9%

Figure 5: Simulated rides versus model. The solid line in each plot gives the power resp. velocity prediction of the model. The prediction errors are analyzed in table. ρ is the correlation coefficient, σ_e is the standard deviation of the prediction error, SNR is the signal-to-noise ratio, and p the percentage of variation explained by the model. In this table the mean error m_e is the predicted average power resp. velocity minus the average measured power resp. velocity.

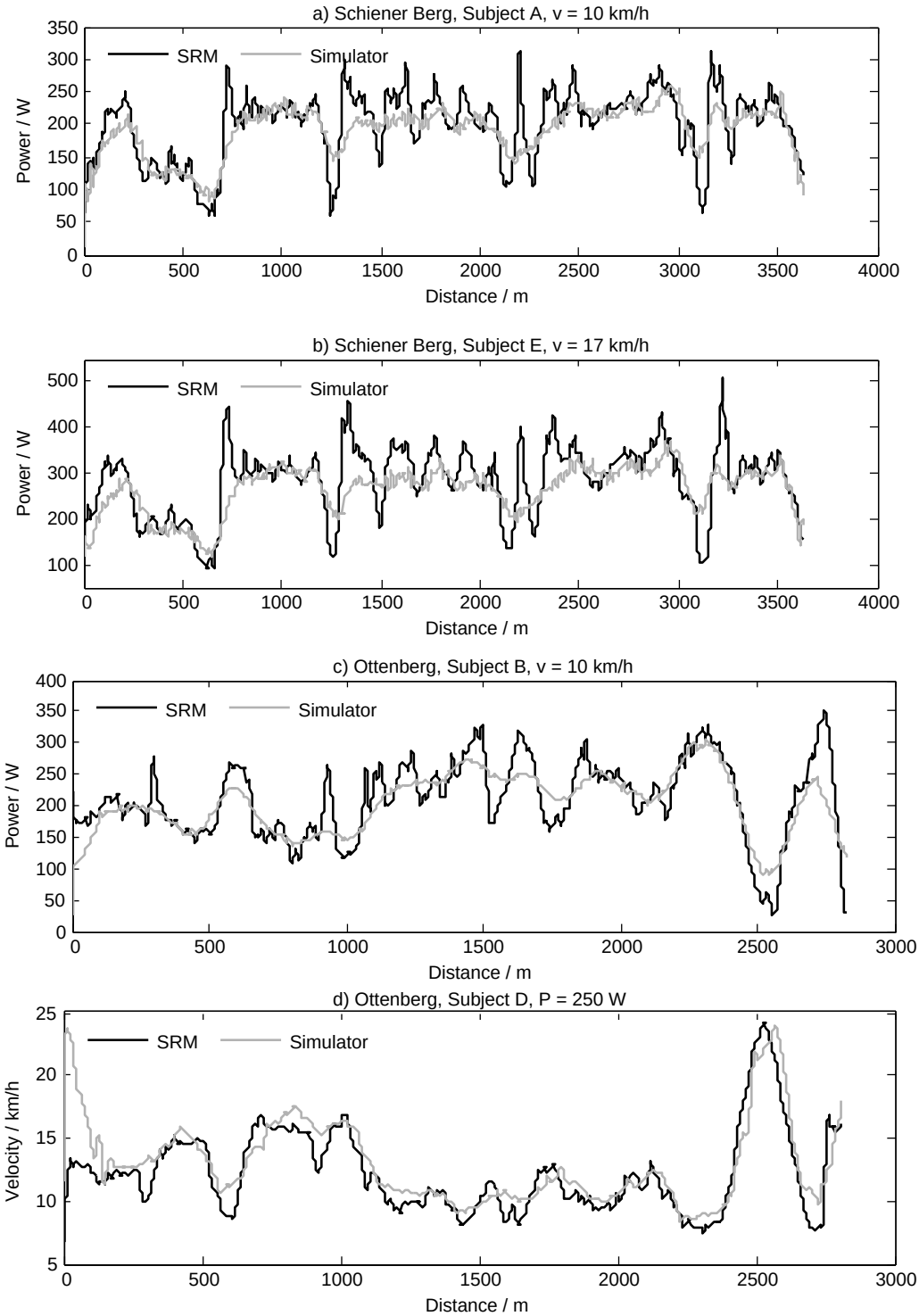

Biker	Condition	Course	ρ	m_e	σ_e	SNR	p
A	$v^\star = 10\,\mathrm{km/h}$	Mountain A	0.70	8.4 W	39.1 W	14.3 dB	96.3%
E	$v^\star = 17\,\mathrm{km/h}$	Mountain A	0.66	19.2 W	58.6 W	13.6 dB	95.6%
B	$v^\star = 10\,\mathrm{km/h}$	Mountain B	0.78	7.4 W	40.0 W	14.7 dB	96.6%
D	$P^\star = 250\,\mathrm{W}$	Mountain B	0.81	-0.02 km/h	0.52 km/h	15.6 dB	97.2%

Figure 6: Field versus simulator rides (for normalised measurements). The differences between real-world and simulator rides are analysed in the table. Mean error is the average measured power resp. velocity in the field minus that on the simulator. The mean error m_e is the average power resp. velocity in the field minus the average measured power resp. velocity with the simulator.

Table 4: Distribution of power for a ride up Schiener Berg (3.63 km, 245 m altitude) at 17 km/h requiring a total time of 12 min 49 s and a total energy of 52.4 Wh.

Power	Average power	Percentage
$\bar{P}_{\text{pot}}$	222.3 W	87.6%
$\bar{P}_{\text{air}}$	17.7 W	7.0%
$\bar{P}_{\text{bear}}$	0.6 W	0.2%
$\bar{P}_{\text{roll}}$	13.2 W	5.2%
$\bar{P}_{\text{kin}}$	0.0 W	0.0%
total	253.8 W	100.0%

power $P^\star$, the velocity was computed. In each case we plotted the computed quantity against the measurement data. Figures 4, 5, and 6 show field measurements and model prediction, simulator measurements and model prediction, and normalised field and simulator measurements, respectively. The tables in Figures 4–6 characterise the deviations of the model predictions from the measurements by giving the correlation coefficient ρ, the mean error m_e, the standard deviation of the error σ_e, the SNR as defined in (14), and the percentage p as defined in (15).

4 Discussion

We organise the discussion in three parts: the comparison of the model predictions with the measurements in the field, with those in the lab, and the comparison of the performance in the field with that in the lab.

4.1 Comparison of measurements in the field with model predictions

The results in Figure 4 show that the mathematical model describes the dynamics of power output on an uphill course with good precision. The signal-to-noise ratio was 18–19 dB, which means that 98 to 99% of the variation of the measured power over the course was accounted for by the model. This finding is even better than the 97% reported in the previous study [8] of Martin et al. We think that this may be due to fact that in the previous study the model was evaluated only for the constant prescribed velocity (on a flat course) while in our study we evaluated the model equations for all of the time steps, thus, also accounting for variations in velocity.

Even though overall the agreement between measurements and model was good there were two types of notable deviations. The first one concerned minima and maxima of power output. At these peaks the model prescribed more moderate values, i.e., the measurements exceeded the prediction. This defect can be attributed to the way the road gradients were computed, namely by Gaussian filtering of a sequence of noisy GPS elevation measurements ($\sigma = 30$ m) followed by finite difference approximation of the slope. The filtering – required to eliminate spurious gradient peaks – also smoothed the natural peaks of the road gradient. This led to the observed smaller model predictions of power at real gradient maxima and larger predictions at minima.

The other notable deviation of the measurements from the model predictions was the large mean error of the predictions, negative for power predictions, and positive for velocity predictions. We believe that this defect may be due to several factors: the physical model parameters may not be sufficiently precise. Some were taken from the literature and should be adapted for our bicycle, the courses, and the riders. Others were measured with errors. Moreover, the model may be incomplete, e.g., we ignored wind effects.

4.2 Comparison of simulator measurements with model predictions

As above for field measurements we have that the measurements of power and velocity on the simulator also agreed well with the mathematical model predictions with a signal-to-noise-ratio ranging from about 17 to 22 dB, see Figure 5. As before, we clearly note differences near peaks and a significant negative mean error of predicted power output. However, in contrast to the above the causes for these artifacts should be explained differently. This is because we cannot blame insufficiencies of the mathematical model for imprecise model predictions since it is the model itself which was implemented in the simulator.

Firstly, unlike above, here we note that the predicted power peaks were more pronounced than the measured ones and not the other way around. We believe that this artifact is due to an insufficiency of the eddy current brake of the ergometer to rapidly react to changing demand in order to produce the required highly variable braking power.

Secondly, the mean error was smaller in magnitude than the error for power predictions in the field, but not equal to zero as expected. This led us to the conjecture of a systematic positive bias in the power as given by the simulator. In order to test this hypothesis, we compared the power measurements of the Cyclus 2 ergometer with those obtained by the SRM system by mounting our bicycle equipped with the SRM system on the ergometer. For example with rider B on the Mountain B with $v^\star = 10$ km/h we obtained a mean power of 195.2 W as measured by the simulator, which was on average 6.5 W *larger* than that simultaneously measured by the SRM (standard deviation was 10.7 W). This clearly confirms our conjecture, as, in fact, the outcome should have been reverse, because the power measured by the SRM at the chain wheel should be larger than that applied to the rear wheel accounting for the losses in the chain and drive system of the bicycle corresponding to the chain efficiency factor $\eta = 0.975$, see Table 1.

4.3 Comparison of simulated rides with outdoor rides

Overall, the performance parameters in the simulations were very similar to those in the field, with a deviation of still 13–15 dB in SNR. See the curves in Figure 6. However, since the SRM power measurements in the field had stronger peaks than the modelled power, which in turn had stronger peaks than the power measurements of the simulator, peaks of field and simulator power measurements differed more strongly. Thus, the variation in power on the simulator was less pronounced than in the field.

5 Conclusions and future work

In this study we confirmed that a mathematical model for performance parameters in road cycling is capable of accurately predicting required power output also on uphill courses with variable road gradients given the location and velocity along with physical, mechanical, and geographical parameters. Alternatively, the model can accurately predict velocity of the cyclist given the power applied at the chain wheel.

We showed that the mathematical model can be implemented on an ergometer for simulated rides on real courses. To a good extent but with certain restrictions the simulation was accurate in modelling the performance parameters on the real courses.

Our study has some limitations; it incorporated (also steep) slopes, but not high velocities, which would test for accuracy of the model regarding higher order terms of the velocity. It did not consider hilly terrain including downhill sections. Furthermore, our results were limited by the accuracy of the required gradients of the courses, which were obtained from noisy GPS elevation data, and by the quality of the other physical and physiological parameters of the mathematical model such as, e.g., the cross-sectional area of a rider.

We conclude the paper with suggested future work. To obtain more accurate road gradients we will consider better estimation methods from noisy elevation data such as Kalman filtering. Also the quality of the elevation data can be improved by more accurate measurements using differential GPS or, from 2014, by the new European satellite navigation system Galileo. Alternatively, commercially available airborne laser scanned elevation data may be used.

To derive improved parameters for the mathematical model we will consider an indirect method. Based on measurements of location, power, and velocity during longer rides over variable terrain we propose to fit the parameters of a generalised model to that data. As a result, we will obtain parameters that act, e.g., as factors for the linear and quadratic terms in the model rather than a complete list of physical parameters. Moreover, in this way we may be able to improve the model by incorporating higher order terms that are not accounted for in the current model.

To improve the operation of our simulator we may redesign its computer control such that the power given by the mathematical model as required at the chain wheel must actually be provided by the rider. This may be achieved by a training procedure to be developed using a feedback loop that includes the SRM measurements at the chain wheel as a control mechanism.

Future work includes measuring also wind direction and velocity both on ground and on the bicycle, simulator rides on terrain with mild hills, so that the downhill parts do not violate the simulator design, i.e, the simulator must still generate a braking force (due to air drag).

We also strive to use the model to find the optimum pacing strategy as Maronski, 1994 [7], Gordon, 2005 [6], and Atkinson, 2007 [2], recently discussed for simple hypothetical height profiles. Together with an extension of physiological measurements and their modelling the whole system shall indicate and train effective tactics using sophisticated biofeedback visualisation and enable cyclists to optimally prepare themselves even for unfamiliar tracks.

Acknowledgements

We thank Dr. Dietmar Lüchtenberg of the Department of Sport Science of the University of Konstanz for discussions and support. A part of this work was carried out while the third author was a Visiting Research Fellow at RSISE, Australian National University, Canberra, whose support is gratefully acknowledged.

References

[1] G. Atkinson and A. Brunskill. Pacing strategies during a cycling time trial with simulated headwinds and tailwinds. *Ergonomics*, 43(10):1449–1460, 2000.

[2] G. Atkinson, O. Peacock, and L. Passfield. Variable versus constant power strategies during cycling time-trials: Prediction of time savings using an up-to-date mathematical model. *Journal of Sports Sciences*, 25(9):1001–1009, 2007.

[3] A. Baca, L. Katz, J. Perl, and O. Spaniol. 06381 abstracts collection – computer science in sports. In Arnold Baca, Larry Katz, Jürgen Perl, and Otto Spaniol, editors, *Computer Science in Sport*, number 06381 in Dagstuhl Seminar Proceedings, Dagstuhl, Germany, 2006. Internationales Begegnungs- und Forschungszentrum für Informatik (IBFI), Schloss Dagstuhl, Germany.

[4] T. Dahmen and D. Saupe. A simulator for racebike training on real tracks. In S. Loland, K. Bø, K. Fasting, J. Halln, Y. Ommundsen, G. Roberts, and E. Tsolakidis, editors, *14^{th} annual Congress of the European College of Sport Science*, Oslo/Norway, June 2009.

[5] P. E. di Prampero, G. Cortili, P. Mognoni, and F. Saibene. Equation of motion of a cyclist. *J Appl Physiol*, 47(1):201–206, July 1979.

[6] S. Gordon. Optimising distribution of power during a cycling time trial. *Sports Engineering*, 8(2):81–90, 2005.

[7] R. Maronski. On optimal velocity during cycling. *J Biomech*, 27(2):205–213, Feb 1994.

[8] J. C. Martin, Douglas L. Milliken, John E. Cobb, Kevin L. McFadden, and Andrew R. Coggan. Validation of a mathematical model for road cycling power. *Journal of Applied Biomechanics*, 14:276–291, 1998.

[9] T. S. Olds, K. I. Norton, and N. P. Craig. Mathematical model of cycling performance. *J Appl Physiol*, 75(2):730–737, Aug 1993.

[10] T. S. Olds, K. I. Norton, E. L. Lowe, S. Olive, F. Reay, and S. Ly. Modeling road-cycling performance. *J Appl Physiol*, 78(4):1596–1611, Apr 1995.

[11] D. Saupe, D. Lüchtenberg, M. Röder, and C. Federolf. Analysis and visualization of space-time variant parameters in endurance sports training. In *Proceedings of the 6th International Symposium on Computer Science in Sports (IACSS 2007)*, 2007.

[12] E Schoberer. Operating instructions for the SRM training system, 1994.

[13] D. G. Wilson. *Bicycling Science, 3rd Edition*. The MIT Press, 3 edition, April 2004.